Journal on Multimodal User Interfaces
https://doi.org/10.1007/s12193-024-00438-9

ORIGINAL PAPER

AirWhisper: enhancing virtual reality experience via visual-airflow multimodal feedback

Fangtao Zhao[1] · Ziming Li[2] · Yiming Luo[3] · Yue Li[4] · Hai-Ning Liang[2]

Received: 1 February 2024 / Accepted: 31 July 2024

Abstract
Virtual reality (VR) technology has been increasingly focusing on incorporating multimodal outputs to enhance the sense of immersion and realism. In this work, we developed AirWhisper, a modular wearable device that provides dynamic airflow feedback to enhance VR experiences. AirWhisper simulates wind from multiple directions around the user's head via four micro fans and 3D-printed attachments. We applied a Just Noticeable Difference study to support the design of the control system and explore the user's perception of the characteristics of the airflow in different directions. Through multimodal comparison experiments, we find that vision-airflow multimodality output can improve the user's VR experience from several perspectives. Finally, we designed scenarios with different airflow change patterns and different levels of interaction to test AirWhisper's performance in various contexts and explore the differences in users' perception of airflow under different virtual environment conditions. Our work shows the importance of developing human-centered multimodal feedback adaptive learning models that can make real-time dynamic changes based on the user's perceptual characteristics and environmental features.

Keywords Virtual reality · Multimodal feedback · Airflow · Human-centered design

1 Introduction

The integration of multimodal user interfaces for immersive technologies, such as Virtual, Augmented, and Mixed Reality (VR/AR/MR), has long been a prominent area of research [1]. In this research area, visual, temperature, olfactory cues, and tactile feedback are often used to create the output modalities in multimodal user interfaces to enhance the user's immersive experience [2, 3]. For tactile feedback, common techniques for providing it involve methods such as vibration [4–6], triboelectric [7], and mechanical transmission [8]. Recently, airflow has emerged as an innovative approach to enhance users' experience in immersive environments, offering distinct features. As a form of non-contact tactile sensation, airflow perception presents an experience that other mediums cannot replicate.

Prior research has suggested that airflow plays an important role in enhancing the user's perception of the environment and can provide richer environmental cues to users [3, 9–12]. As a kind of non-contact haptic feedback, airflow is detected by multiple tactile receptors, such as velocity and spatial intensity, giving them advantages that other conventional tactile feedback modalities do not have, e.g., vibration [13] and thermal [14]. In addition, recent research has shown that airflow has a role beyond simulation. The external airflow can reduce simulator sickness in VR [15–19] and lead to higher subjective feeling of social presence [20]. In short, this prior research demonstrates a broader application of airflow-based modality to enhance users' experiences in VR or MR.

Although some past studies [15, 16, 19, 21] have not addressed airflow variability in virtual environments, more and more researchers [14, 17, 20, 22–24] are making airflow variability an important aspect of its use. However, to our knowledge, none of them have systematically investigated the characteristics of people's perception when airflow

✉ Hai-Ning Liang
hainingliang@hkust-gz.edu.cn

1 Department of Computer Science, University of Southern California, Los Angeles, USA

2 Computational Media and Arts Thrust, The Hong Kong University of Science and Technology (Guangzhou), Guangzhou, China

3 School of Cyber Engineering, Xidian University, Xi'an, China

4 School of Advanced Technology, Xi'an Jiaotong-Liverpool University, Suzhou, China

Published online: 20 August 2024

is adjusted dynamically in VR environments and multimodal interfaces, leaving a gap that needs to be filled. In this paper, we comprehensively analyze the characteristics of the user perception of changes in airflow when designing a dynamic airflow-based feedback interface and use it in a study to evaluate its effect on users' experience in two VR scenarios.

In this research, we focused on a user-friendly device that is relatively easy to attach to a VR head-mounted display (HMD), is safe to use, has low-cost components, and provides realistic wind-based feedback to address the gap in using wind as an additional modality for enhanced VR experiences. To this end, we developed AirWhisper (see Fig. 1), a compact and modular wearable device that seamlessly integrates with an HMD. It can provide dynamic airflow from four distinct directions around the user's head, utilizing four micro fans equipped with 3D printed attachments. When AirWhisper is attached to an HMD, we combine visual feedback and wind feedback to form a multimodality output. We measured the performance improvement of this multimodality output over the single modality output via a user study. Then, we conducted another user study based on a practical application to measure improvements in user experience.

In summary, we make the following contributions:

- We designed a novel device that effectively integrates with VR to create a visual-haptic multimodality output, enhancing the overall user experience.
- We evaluated the performance of our device and showed that it could complement other feedback modalities and improve users' experience in VR in various scenarios.
- We systematically explored how airflow feedback devices should be designed to integrate with VR devices to provide user-friendly multimodal output.

2 Related work

2.1 Visual-haptic multimodality output in virtual reality

Visual-haptic multimodality output integrates visual and haptic feedback mechanisms within VR environments to enhance users' interaction and their feeling of immersion and realism [5, 6, 25, 26]. This integration allows a more complete sensorial experience. In 1996, Burdea et al. [27] provided foundational insights into multimodal interactions in VR, emphasizing the integration of special-purpose input–output devices. Subsequently, the visual-haptic multimodality has continuously remained a focal point of research in VR. Yokokohji et al. [28] developed a WYSIWYF display combining vision-based tracking and haptic devices for realistic, spatially, and temporally consistent visual-haptic integration. Schwind et al. [29] explored how the appearance of virtual hands affects visual-haptic integration, offering insights into multi-sensory integration in VR. Gibbs et al. [30] investigate how haptic and visual feedback separately and combined affect users' sense of presence in a VR environment, finding that presence is enhanced with both types of feedback, with a strong suggestion that haptic feedback alone may enhance presence more than visual feedback alone. Wu et al. [31] developed a VR-based table tennis training system using visual, haptic, and temporal cues, demonstrating significant skill improvements and enhanced understanding of spin shots in users. Collectively, these studies not only delineate the current state of visual-haptic output in VR but also pave the way for future explorations to augment user experiences through improved multimodal interactions and haptic technologies.

2.2 Airflow feedback devices

Airflow has a variety of applications in VR and has proven to have great potential. On a large scale, Hlsmann et al. [21] proposed a system to simulate winds and temperatures in a well-designed three-sided CAVE. Using small fans and cube-connected structures, Moon and Kim [22] introduced a wind display system called the "WindCube". For mid-air interfaces, Sodhi et al. [32] introduced "AIREAL" which uses the pressure difference inside the air vortex to generate tactile sensation. Tsalamlal et al. [33] proposed non-invasive tactile stimulation to different and large areas of the human body using a tactile stimulation strategy based on mobile air jets. Additionally, recent studies have established the significant role of external airflow in mitigating simulator sickness [15–19] and increasing subjective perceptions of social presence [20] in VR environments, underscoring its importance beyond traditional simulation applications. This prior work illustrates the wide range of applications for airflow-based multimodality output, highlighting the importance of studying human airflow perception.

Prior work also showed that users favored head-mounted mobile wearable devices, which can provide richer feedback for VR experiences. These devices incorporate a number of different technological approaches to create various types of stimulation. As for the airflow-based modality output, Ambiotherm [14] provided thermal and wind stimulation to stimulate realistic environmental conditions and compared four types of sensory information (Ambiotherm, VR+Thermal, VR+Wind, and normal VR). The wind simulation module in Ambiotherm focusing on the user's front face has achieved good performance, though it can only simulate the wind blowing from the front of users' heads. Another prototype is VaiR [23]. It emits airflow with minimal delay and animates air sources in the 3D space around the user's head. The weight of the VaiR helmet is successfully controlled to be low. However, a 4 kg backpack is required for

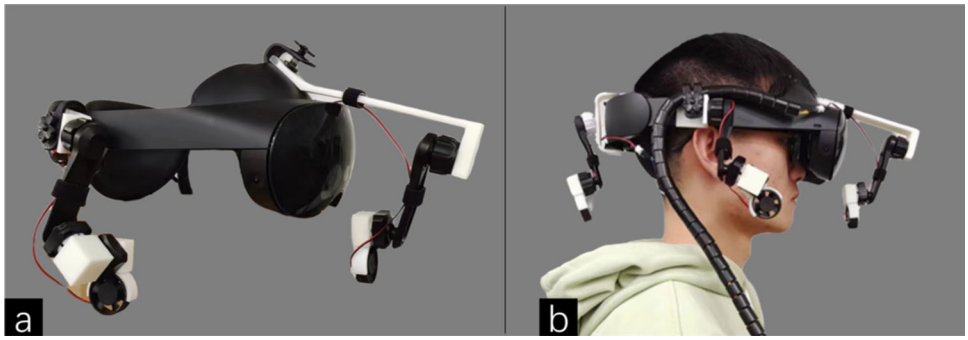

Fig. 1 **a** The AirWhisper prototype, which can provide continuously changing airflow feedback integrated with the VR headset. **b** A user wearing AirWhisper and immersed in a VR environment

the compressed air bottle, making it impractical for many scenarios. HeadWind, developed by Tseng et al. [24], simulates the haptic sensation of air drag when rapidly moving through the air in real life to improve the experience of teleportation in VR, indicating a new application of airflow. Similarly, Liu et al. [34] presented HeadBlaster, an innovative wearable technology that induces motion perception by using jets to apply ungrounded forces to the head, stimulating the vestibular and proprioceptive systems.

Existing research on airflow-based modality output in VR mainly explores specific applications focusing on device usability. Our work aims to broaden this scope by systematically studying how users perceive airflow in different situations. This human-centered approach seeks to inform the design of future airflow-based modality output across various applications.

2.3 Just noticeable difference studies in dynamic haptic interface design

Defined as the smallest detectable difference in intensity or stimulation between two stimuli recognizable by an individual, Just Noticeable Difference (JND) has become essential in psychological and sensory studies to provide insights into people's perception of gradual changes [25, 35]. JND analysis has been extensively applied to the design of haptic interfaces to find the intensity of haptic feedback that meets the user's perceptual characteristics, reflecting a more human-centered design approach. In a study on VR multimodal perceptions over wireless cellular networks, [36] utilized the JND measure to compare orthogonal and non-orthogonal slicing methods for visual and haptic perceptions. Lee et al. [37] conducted a study to determine quantitatively the JND of visual-proprioceptive conflict in VR and to assess whether cutaneous haptic feedback can further reduce this conflict. Tsai et al. [38] conducted a JND study to assess the distinguishability of impact force levels in three axes on the head. Junput et al. [39] utilized a JND study to determine the minimum variation in virtual object stiffness that participants could perceive, thereby assessing the effectiveness of their vibrotactile feedback glove in simulating realistic haptic sensations in VR environments. Ryu et al. [40] conducted a JND study to measure users' perception of varying stiffness in flexible objects held and shaken in the hand, addressing a gap in the literature where no previous studies had described human perception of stiffness variation in this context. However, studies explicitly addressing JND in the context of airflow perception are markedly lacking, revealing a notable gap in this area. With a human-centered focus, we pose the following research questions to frame our work:

RQ1: How does the strength or size of the airflow affect users' perception of the airflow?
RQ2: How does the direction of the airflow affect users' perception of the airflow?
RQ3: How does a mixed interface of visual and airflow cues affect users' perception of airflow in VR?
RQ4: How does the changing patterns of airflow affect users' perception of airflow in VR?
RQ5: How does the interactivity of the scene affect users' perception of the airflow in VR?

3 Implementation

In this section, we introduce AirWhisper, an airflow-based haptic device designed to enhance immersive experiences with virtual reality head-mounted displays. Several considerations guided the development of AirWhisper:

- *Wearability and Portability.* Wearability and portability were priorities to allow freedom of movement within virtual environments. Bulky equipment such as large fans [41], air compressors [42], or compressed air canisters [23] would not suffice. Instead, micro fans were chosen for their small size and mobility. The device uses an adjustable structure rather than fixed supports to position air supply units, allowing for personalized adjustment.
- *Modularity.* Modularity was also important so the device could function as an optional accessory. Not all VR experiences involve airflow, so users can easily attach and detach the device as needed.

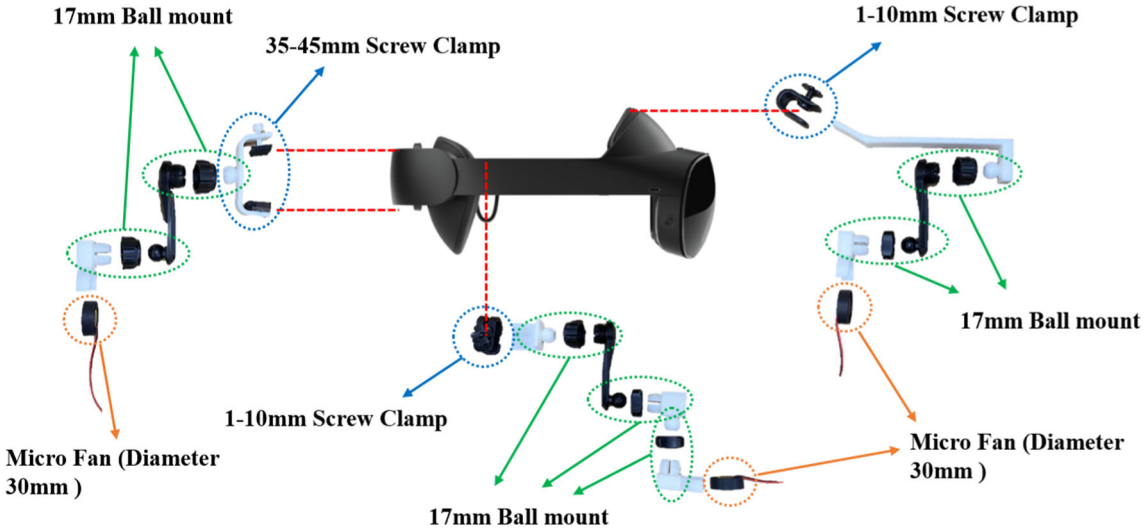

Fig. 2 The hardware structure and components of AirWhisper. The red line indicates the connecting parts. While this version is based on a Meta Oculus Quest Pro, it could also be adapted to other types of HMDs

- *Low-cost.* Low production cost was a goal to make AirWhisper affordable for widespread adoption. This influenced the selection of lightweight and inexpensive components and materials.
- *Feedback Realism.* Realistic wind simulation was prioritized by positioning airflow near the neck and cheeks, highly sensitive areas [43]. The adjustable structure, instead of fixed positioning, allows users to customize feedback locations based on individual perception differences and airflow characteristics, optimizing the experience.

Based on these considerations, the development of AirWhisper prioritized a balance between advanced functionality and cost-effectiveness. The device consists of several key components, including micro fans, 3D-printed supports, adjustable ball joints, and control electronics. Despite its sophisticated design, careful selection of materials and manufacturing techniques has kept the overall cost low. The estimated material cost for each AirWhisper unit ranges between $50 and $70. This cost-effective approach ensures that AirWhisper is accessible for wider adoption without sacrificing performance or reliability.

The design complexity is managed through a modular and adjustable structure, allowing for personalized configuration without the need for specialized tools or equipment. The integration of micro fans with ball joints and adjustable arms ensures that airflow can be precisely directed to enhance the user experience. Additionally, the simplicity of the system's assembly and control minimizes the potential for mechanical failure, ensuring durability and ease of maintenance. The detailed design of each part is discussed below.

3.1 Design of airflow units

AirWhisper contains four adjustable airflow units (see Fig. 2). Each unit holds a micro fan inside a 3D-printed semicircular clasp. A 17 mm ball head base connects the clasp to a supporting arm through a ball joint for positioning flexibility. Two types of supporting arms are designed based on the original HMD structure–one for the front and another for the back and sides. The front arm attaches via a clamp, while the back/sides use a different clamp design. Additional ball joints are incorporated to enable directional adjustment of each supply unit further.

Special considerations were made for the front components near the original sensors and cameras. The supply units are kept at a distance to avoid interfering with functions like transparency mode and facial recognition. The front supporting arm attaches to the rigid external skeleton near the HMD-head interface to position the center of gravity similarly to the original HMD design. A partially inclined plane matches the curvature. The left and right supporting arm designs are identical due to the HMD's symmetry. Each connects a supply unit to the back of the external skeleton on the respective side. Iterative adjustments were made to the attachment points to align the overall center of gravity more optimally. 90-degree joints with ball heads enable side-to-side positioning. The back supporting arm uses the same design as the sides and attaches via a sized clip. Testing revealed clashes between back components and users' hair/collars, so distance from the head is maintained to prevent discomfort or safety issues.

Overall stability is retained with the center of gravity closely matching the original HMD design. The total additional weight is 303 g, excluding wiring (front: 82 g, back:

58 g, left: 81.5g, right: 81.5g). Pilot assembly/disassembly testing showed most participants could complete the process within 2 min after 5 min of training.

3.2 Airflow control mechanisms

After showing that the system could be set up easily, we next conducted a pilot test to examine the generated airflow strength at various distances from the micro fans. As shown in Fig. 3, the airflow speed remained consistent within a range of 5–7 cm (236–216ft/min, with less than 10% variation), indicating distance variations within this span had minimal influence. Therefore, airflow strength could be controlled primarily by adjusting the applied voltage.

AirWhisper utilizes four independent airflow supply units regulated through the four ports of an Arduino UNO board, which can output 0-5V per port. The Arduino contains an 8-bit analog-to-digital converter (ADC) capable of representing 256 different values. Rather than directly measuring airflow speed, which is difficult, we use this 256-unit scale where 0 represents 0V and 255 represents 5V, with each unit equivalent to approximately 0.0196V. Unity reads the ADC values via stable serial communication rather than unreliable Bluetooth. An adjustable 0-12V power supply divides the voltage among the four units through a four-channel MOSFET for independent control of each.

3.3 Calibration of control parameters

After examining the setup, a JND user study was used to explore the range of output regulation of the wind control units. The purpose of the study was to find the specific values that would be perceived by most users as low, medium, and strong wind output levels (will be represented as level 1, level 2, and level 3, respectively) and how much voltage output would be required from the control units (RQ1). Furthermore, this study will simultaneously explore the user's optimal wind feedback intensity for all four directions: front, back, left, and right (RQ2).

Twelve (12) participants (7 males and 5 females) aged 20-26 (median 23) were recruited for this study. All sensory functions were normal in all participants. They were compensated with snacks and drinks for their time.

3.3.1 Task and procedure

The experimental procedure followed a traditional JND study design with some modifications to suit our airflow devices. Participants were seated upright and still, looking straight ahead. For each trial, they received two 3-second airflow stimuli sequentially and reported whether the intensity was the same or different. A 3-second inter-stimulus interval prevented residual sensation carryover. A pilot study established a comfortable range of 0-210 units for stimuli intensities at 25 °C ambient temperature. The base intensity values tested were 25, 50, 75, and 100 units, while offset increments were 0, 8, 16, and 24 units. This produced 16 intensity pair conditions across the four directions–front, back, left, and right. Each participant, therefore, completed 64 trials (4 directions x 16 pairs). The trial order was determined using a Latin square design to counterbalance learning effects. Overall, the study duration was approximately 20 min.

3.3.2 Results

Figure 4 quantitatively presents the results of the JND study, showing perceptual sensitivity to changes in airflow direction from front, left, back, and right.

For front airflow, participants most easily detected an offset of 24 units from the highest 100 base level, with 92% sensitivity. However, the detection was less consistent at lower bases, hovering around 25–58% for 8–16 units of offsets.

Lateral airflow perception showed a more gradual improvement in detection corresponding to increased offset values across bases. Notably, 83% of participants discerned 24 units for the left offset from 100 units and 92% for the right offsets under the same conditions.

Back airflow demonstrated the highest sensitivity, with 100% detection of changes even at the strongest test point. Detection rates from the back were also consistently higher than front or lateral airflow across all conditions.

In summary, sensitivity to airflow variations followed an order from $back > right \approx left > front$. The perception was most precise for back airflow intensity changes. Front airflow required larger variations to be reliably detected compared to other directions. Overall, the JND thresholds provided empirical calibration guidelines for the haptic control system.

3.3.3 Final design

The results showed participants' ability to perceive changes in airflow intensity varied depending on the direction. To ensure consistent resolution across all feedback conditions, the default control parameters were selected based on high accuracy levels uniformly achieved across different directions. Specifically, a base level of 75 units with an offset of 24 units was chosen as it elicited over 80% accurate change detection in all tested directions. This combination provided reliable perceptibility of variations while avoiding excessive offset magnitudes that may cause discomfort. These calibrated parameters informed the implementation of three discrete intensity levels–level 1 at 51 units (base-offset), level 2 at the base of 75 units, and level 3 at 99 units (base + offset) - for the subsequent virtual reality experience study. Based

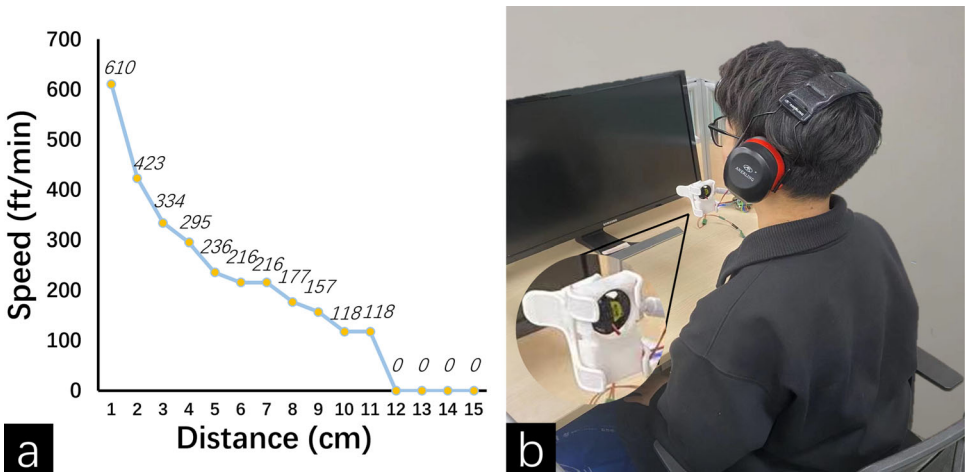

Fig. 3 **a** Airflow strength generated by the micro fan at different distances. **b** A participant was performing the airflow perception experiment

Base

Offset	25	50	75	100
0	0.25	0.25	0.58	0.17
8	0.42	0.25	0.33	0.42
16	0.42	0.58	0.58	0.75
24	0.58	0.75	0.92	0.92

Front

Base

Offset	25	50	75	100
0	0.25	0.33	0.42	0.08
8	0.33	0.42	0.50	0.33
16	0.33	0.75	0.67	0.67
24	0.83	0.92	0.83	0.58

Left

Base

Offset	25	50	75	100
0	0.08	0.42	0.50	0.25
8	0.50	0.25	0.42	0.42
16	0.50	0.75	0.67	0.58
24	0.83	0.92	1	0.92

Behind

Base

Offset	25	50	75	100
0	0.17	0.17	0.25	0.25
8	0.42	0.33	0.50	0.33
16	0.25	0.67	0.75	0.67
24	0.33	0.58	0.92	0.83

Right

Fig. 4 Airflow perception study results. The score represents the percentage of users who think the airflow strength is different

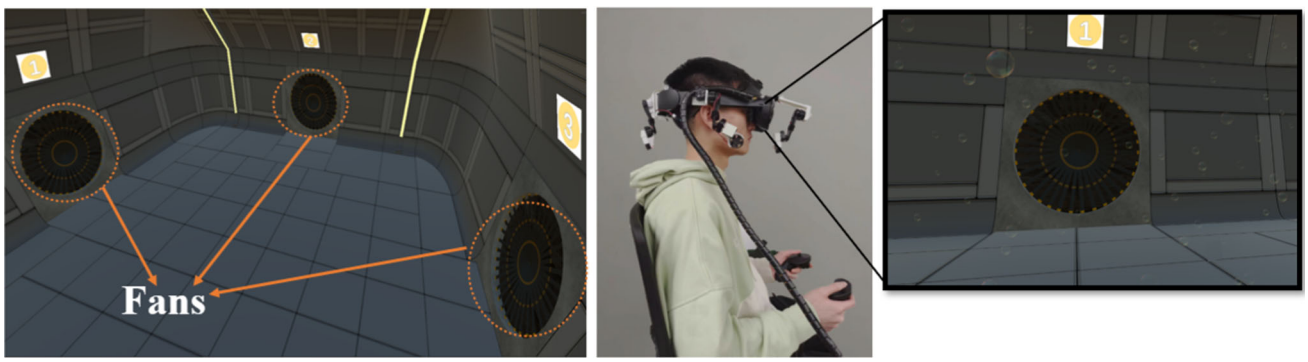

Fig. 5 The apparatus and VR scene of the evaluation study. Four wind sources were placed around the user to provide airflow from different directions

on the above results, we completed the system construction of the control units.

4 Study 1: Comparing vision-airflow multimodality output and single modality output

In study 1, we aim to explore the variation in performance of the vision-airflow multimodality output we constructed above compared to the single modality output of vision and airflow (RQ3). To achieve this aim, our research introduces a sensory comparative experiment designed to evaluate the human perception of airflow in various directions under three modality output conditions: (1) vision, (2) airflow, and (3) vision-airflow. We analyzed the accuracy, task load, and usability of the system in different conditions. This experimental setup allows us to thoroughly assess the accuracy, cognitive load, and usability of the system under each sensory condition, thereby providing a nuanced understanding of multimodality integration in the perception of airflow.

We recruited 24 participants (13 males and 11 females) aged 19–25 years (median 21). All sensory functions were normal in all participants. Eight of them had no experience with VR before.

4.1 Feedback methods

For vision output, we used the wind zone to create a virtual airflow environment in the scene, cooperating with a particle system using material simulating transparent bubbles to avoid overloading the visual sense. Four sets of particle effects were placed in front of, behind, left of, and right of the participant, but only particles in the measured direction activated at one time, together with corresponding changes in wind zone direction, to provide vision feedback in VR. The wind zone was set to directional mode. Airflow levels (1, 2, 3) corresponded to (64, 256, 1024) units in Unity. For airflow feedback, we used AirWhisper as described previously. Based on the results of the JND study, airflow levels (1, 2, 3) were (51, 75, 99) units. We also examined simultaneous vision and airflow feedback, the most likely approach for future applications. The feedback intensity was the same as above.

4.2 Task and procedure

Participants sat on the chair and experienced a designed VR scene with vision-airflow multimodality output, as shown in Fig. 5. They were required to wear earphones playing pink noise to mask sounds from the experimental equipment and external environment.

In the VR scene, we positioned four fans in front of, behind, left of, and right of the participant. In each task, participants experienced a certain airflow level from one direction. Each 5-second stimulus was followed by a selection page with three buttons (1, 2, 3) for participants to indicate their perceived level. After selection, click 'Next' to begin the next trial. An extra 3-second loading page between stimuli prevented residual sensation.

Before the official start of the experiment, participants had 10 min to explore the VR scenario and each condition in all directions. A control menu allowed the selection of any sensory mode, direction, and airflow level. Calibration also preceded each condition, so sensations did not need to be memorized. The airflow level was randomized based on a Latin matrix, but stimuli from the same direction were tested continuously so participants could focus on the airflow level without spending effort on direction judgment. In each direction, the first three trails are calibrated at levels 1, 2, and 3 in order, followed by six formal trials (3 levels $\times$ 2 repetitions) given randomly.

Each participant needs to complete 72 trials (4 directions $\times$ 3 sensory modes $\times$ 3 airflow levels $\times$ 2 repetitions). After each sensory mode, participants were asked to complete two questionnaires, NASA-Task Load Index (NASA-TLX) [44] (6 items for cognitive load, e.g., "mental/perceptual activity required") and System Usability Scale (SUS) [45] (10 items, e.g., "frequency of future use"). The full experiment lasted 50 min, including introduction, rest, and filling out questionnaires.

4.3 Results

All participants in this experiment understood and completed the given experimental tasks successfully. The data we collected were valid. As the results of the Shapiro-Wilk test showed that the objective data we collected during the experiment were not normally distributed ($p < .05$), we used the Friedman test to analyze the objective data. Following that, we conducted the Wilcoxon signed-rank post hoc test. Similar to the objective data, we used the same method to analyze the subjective data.

4.3.1 Objective results

We divided the total number of tests by the number of correct tests to get the accuracy value (from 0 to 1) for each trial. Then, the Shapiro-Wilk and the Wilcoxon signed-rank tests were used to analyze the difference between the accuracy under the three feedback modes. The Shapiro-Wilk test determined that the accuracy value differed statistically significantly between the feedback mode in the right direction ($X^2(2) = 13.80, p < 0.05$) and the left direction ($X^2(2) = 16.77, p < 0.05$). However, there were no sig-

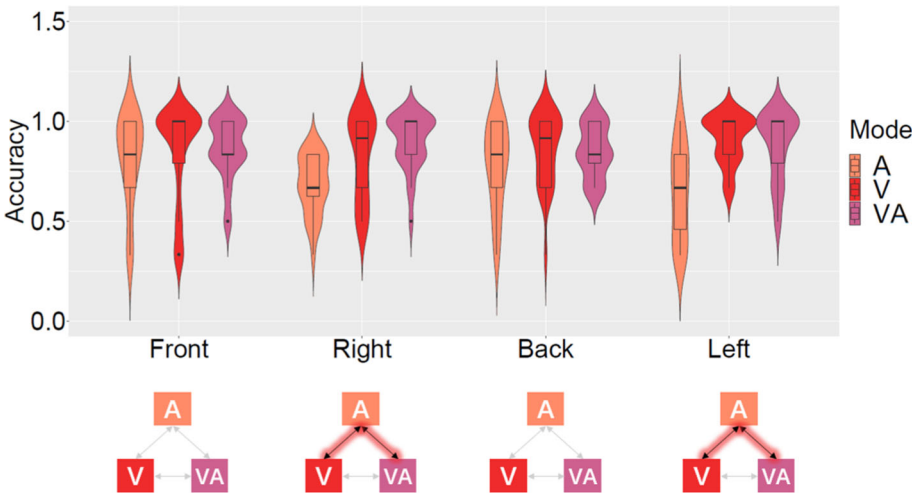

Fig. 6 Accuracy analysis results in the perception study. Bold two-way arrows indicate statistically significant differences between the two modes. A: airflow-only feedback mode. V: vision-only feedback mode. VA: airflow with vision feedback mode

nificant differences between the front direction ($p > 0.05$) and the back direction ($p > 0.05$). For the right direction, the median (IQR) accuracy values for the airflow-only feedback mode, vision-only feedback mode, and airflow with vision feedback mode were 0.67 (min = 0.33, max = 0.83, SD = 0.15), 0.92(min = 0.50, max = 1.00, SD = 0.21) and 1.00 (min = 0.50, max = 1.00, SD = 0.14), respectively. As a further step, the Wilcoxon signed-rank test revealed that the accuracy value under airflow-only feedback mode was significantly lower than the accuracy under vision-only feedback mode ($Z = -2.23$, $p < 0.05$), and the accuracy under airflow with vision feedback mode ($Z = -3.57$, $p < 0.05$). As for the left direction, the median (IQR) accuracy values for the airflow-only feedback mode, vision-only feedback mode, and airflow with vision feedback mode were 0.67 (min = 0.33, max = 1.00, SD = 0.23), 1.00 (min = 0.67, max = 1.00, SD = 0.12) and 1.00 (min = 0.67, max = 1.00, SD = 0.17), respectively. The post hoc test found the accuracy value under airflow-only feedback mode was significantly lower than the accuracy under vision-only feedback mode ($Z = -3.72$, $p < 0.05$), and the accuracy under airflow with vision feedback mode ($Z = -2.92$, $p < 0.05$). Figure 6 summarizes the above results.

4.3.2 Subjective results

During the experiment, all participants were asked to complete two questionnaires, the NASA-TLX and the SUS. We conducted the Friedman Test to analyze the data and the Wilcoxon signed-rank test for the post hoc analysis.

Figure 7 shows the summary of the NASA-TLX data. The results showed that when participants were under different feedback conditions, statistically significant effects could be found in all six elements of workload, mental ($X^2(2) = 11.58$, $p < 0.05$), physical ($X^2(2) = 7.12$, $p < 0.05$), temporal ($X^2(2) = 7.54$, $p < 0.05$), performance ($X^2(2) = 6.16$, $p < 0.05$), effort ($X^2(2) = 6.89$, $p < 0.05$), and frustration ($X^2(2) = 12.69$, $p < 0.05$). Furthermore, the post-test shows that compared to the participants under airflow-only feedback mode condition, the values of mental ($Z = -3.22$, $p < 0.05$), physical ($Z = -2.91$, $p < 0.05$), temporal ($Z = -2.54$, $p < 0.05$), performance ($Z = -2.29$, $p < 0.05$), effort ($Z = -2.64$, $p < 0.05$), and frustration ($Z = -3.22$, $p < 0.05$) were lower in the airflow with vision feedback mode condition. While compared to the participants under vision-only feedback mode condition, the values of mental ($Z = -2.41$, $p < 0.05$), effort ($Z = -2.30$, $p < 0.05$), and frustration ($Z = -2.40$, $p < 0.05$) were lower in the airflow with vision feedback mode condition. These results indicate that of the three feedback modes, participants had the lowest workload demands in airflow with vision feedback modes.

Figure 8 shows the participants' SUS scores for the systems equipped with different feedback modes. The results show that there was a significant difference in the SUS scores when the participants were under different feedback conditions ($X^2(2) = 13.57$, $p < .05$). Furthermore, the post-test shows that there was a statistically significant reduction in the airflow with vision feedback mode vs. airflow-only feedback mode ($Z = -3.51$, $p < .05$) and in the airflow with vision feedback mode vs. the vision-only feedback mode ($Z = -2.49$, $p < .05$). These results indicate that the participants prefer to use the system equipped with airflow and vision feedback mode.

4.4 Summary

This study investigated the effects of single versus multimodal feedback on spatial perception, cognitive load, and user experience in virtual reality environments. Participants completed experimental tasks under vision-only,

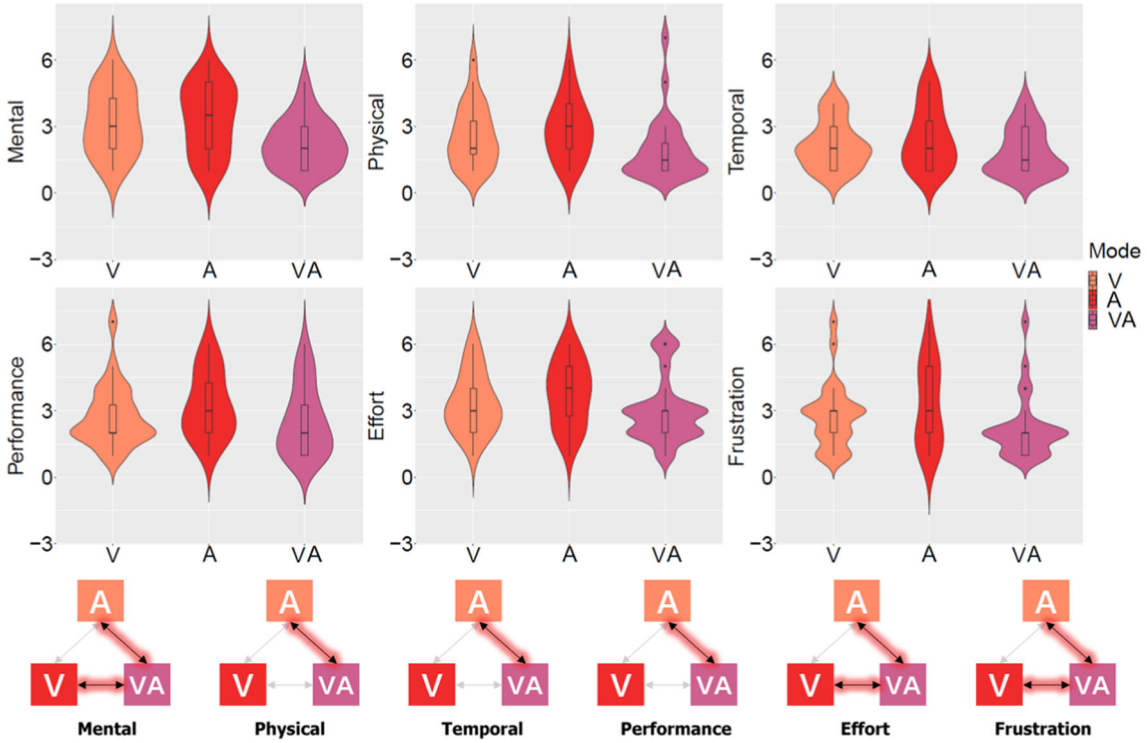

Fig. 7 Average of response scores for each element of NASA-TLX workload. Bold two-way arrows indicate statistically significant differences between the two modes. A: airflow-only feedback mode. V: vision-only feedback mode. VA: airflow with vision feedback mode

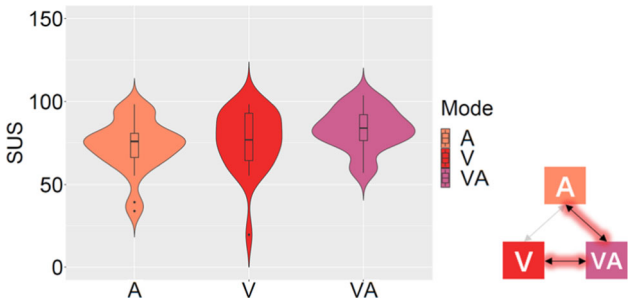

Fig. 8 System usability analysis results in perception study. Bold two-way arrows indicate statistically significant differences between the two modes. A: airflow-only feedback mode. V: vision-only feedback mode. VA: airflow with vision feedback mode

airflow-only, and integrated vision-airflow feedback conditions generated by the AirWhisper haptic device.

A primary finding was variation in airflow perception accuracy based on direction. Front and back airflow was consistently detected, while lateral airflow proved more difficult to identify using airflow-only feedback. However, the addition of visual cues drastically improved left and right accuracy, highlighting the synergy between senses.

In the case of integrating visual feedback into the overall feedback system, that is, blending wind feedback to form multimodal feedback, participants' cognitive workload was also reduced, and their preference was increased. This likely stems from the natural ease of holistically processing congruent information from multiple senses simultaneously. The cognitive benefits, in turn, enhance immersion and enjoyment. Notably, all participants could perceive and report on various intensities from the JND-calibrated control system, validating its resolution design.

In conclusion, the vision-airflow multimodal feedback integrated by AirWhisper significantly enhanced spatial perception, cognitive functioning, and overall user experience in virtual environments relative to single feedback methods.

5 Study 2: Evaluating the usability of the vision-airflow multimodality output

Building on the findings of the first study, Study 2 aimed to evaluate AirWhisper's ability to provide dynamic, real-time haptic feedback corresponding to virtual experiences. Four airflow feedback conditions were tested: 1) no airflow, 2) constant airflow, 3) linearly changing airflow, and 4) step-changing airflow (RQ4). Furthermore, to assess user experience under varying levels of environmental interactivity, two generic VR scenarios were constructed - a passive rollercoaster ride and an interactive motorcycle driving experience (RQ5). Both offered first-person perspectives for immersion.

Participants underwent trials with each airflow condition applied in both scenarios. Feedback was collected regarding their perception of and engagement with the airflow variations. Comparisons across conditions and scenarios aimed to provide insight into how environmental interactivity may influence humans' capacity to detect and comprehend changing airflow cues integrated with virtual activities in real time. By systematically manipulating the feedback method, content, and interactivity level, this study delivered a more holistic evaluation of AirWhisper's performance from the user experience perspective.

Twelve (12) participants (8 males, 4 females) aged 20-26 years (median 22) were recruited in this study. All had some prior experience with VR, with six having extensive experience with it.

5.1 Study settings

5.1.1 Airflow feedback settings

Four different airflow feedback types were set for the two application scenes: (1) no airflow, (2) constant airflow, (3) linear-changing airflow, and (4) step-changing airflow. The airflow conditions in the last three types were provided by AirWhisper. For airflow control methods, the airflow intensity (A) is treated as a dependent variable, while the moving velocity in a virtual environment (V) is the independent variable. The range of A is set to [0, 200] to ensure safety and comfort, and the range of V is set to [0, 10] for the same reason. For the three methods with airflow, we define a minimum velocity threshold T_0 such that airflow is provided only when the velocity exceeds this threshold.

Under the **Constant airflow** type (Fig. 9a), the intensity remains fixed at a value of 100 units once the velocity exceeds the minimum threshold:

$$A = \begin{cases} 0 & \text{if } V < T_0 \\ 100 & \text{if } V \geq T_0 \end{cases}$$

Under the **Linear-changing airflow** type (Fig. 9b), as the virtual velocity V increases, the airflow intensity A increases proportionally:

$$A = \begin{cases} 0 & \text{if } V < T_0 \\ kV - b & \text{if } V \geq T_0 \end{cases}$$

where k is the coefficient that maps the virtual velocity isometrically to the airflow intensity, and $\frac{b}{k} = T_0$ (minimum velocity threshold).

Under the **Step-changing airflow** type (Fig. 9c), the airflow intensity remains constant until it reaches certain virtual velocity thresholds, where it increases abruptly to new fixed levels. In addition, according to the results of the JND Study, the human airflow perception aligns with the Weber-Fechner law in psychophysics; therefore, larger increments are required for higher intensity. We applied three step values L_1, L_2, L_3 ($L_1 < L_2 < L_3$), and each promotion was twice the value of the previous promotion ($4 \times (L_1 - 0) = 2 \times (L_2 - L_1) = (L_3 - L_2)$):

$$A = \begin{cases} 0 & \text{if } V < T_0 \\ L_1 & \text{if } T_0 \leq V < T_1 \\ L_2 & \text{if } T_1 \leq V < T_2 \\ L_3 & \text{if } V \geq T_2 \end{cases}$$

where T_1, T_2 are the designed changing thresholds with $T_1 < T_2$.

To measure the user experience in the virtual environment, we used a modified version of the presence questionnaire (PQ) [46] (19 items for non-interactive scenes and 23 items for the interactive scenes, such as "How compelling was your sense of moving around inside the virtual environment?") and the enjoyment questionnaire (enjoyment component from E^2I Questionnaire [47]) (4 items, such as "To what degree did you feel sad when the experience was over?"). We also measured the simulator sickness using the simulator sickness questionnaire (SSQ) [48] (16 items, such as "General discomfort"). At the end of the experiment, participants were interviewed to get further feedback and additional comments.

5.1.2 Settings of the VR scenarios

We developed two VR scenarios using Unity: roller coaster (non-interactive) and motorcycle riding (interactive), as shown in Fig. 10. In the first application, the user sat in the front row of a roller coaster on a pre-designed track, including climbs, drops, and inversions, in an open grassy area without distractions. As this was non-interactive, the user focused on the feedback without needing to control anything. The second interactive application required the user to drive a motorcycle for a full lap as quickly as possible. The track contained low/high-speed turns and straights without other vehicles or obstacles. Here, users focused on controlling the motorcycle using right/left triggers for acceleration/brake and the left joystick for steering.

5.2 Task and procedure

First, participants were briefed on the study and the experimental procedure. Then, they were introduced to the AirWhisper prototype, HMD, and controllers and were given the chance to try them out. Participants were free to observe the structure of the prototype and adjust the movable joints to help them become familiar with the devices. In the first scene, riding a roller coaster, participants sat in a chair and wore the

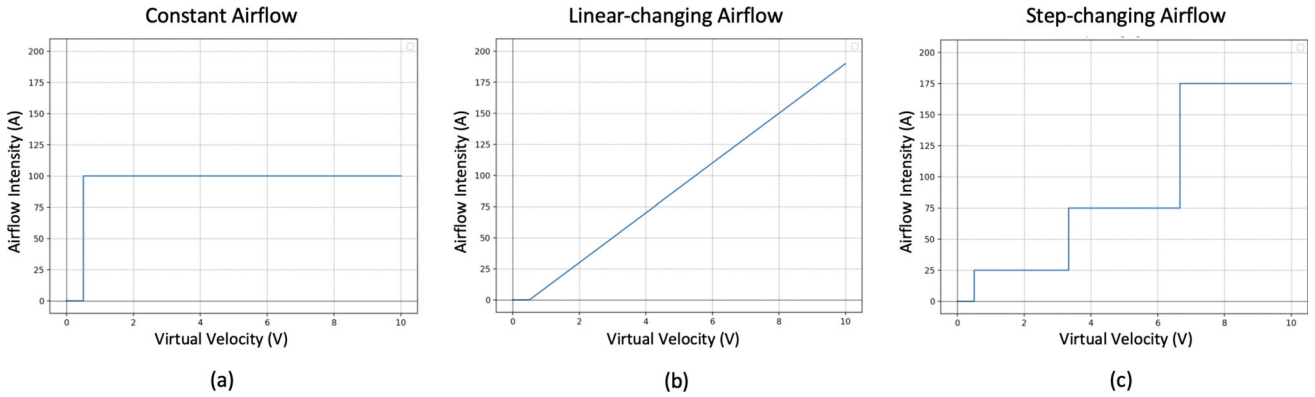

Fig. 9 Three airflow changing methods: **a** Constant airflow, **b** Linear-changing airflow, **c** Step-changing airflow

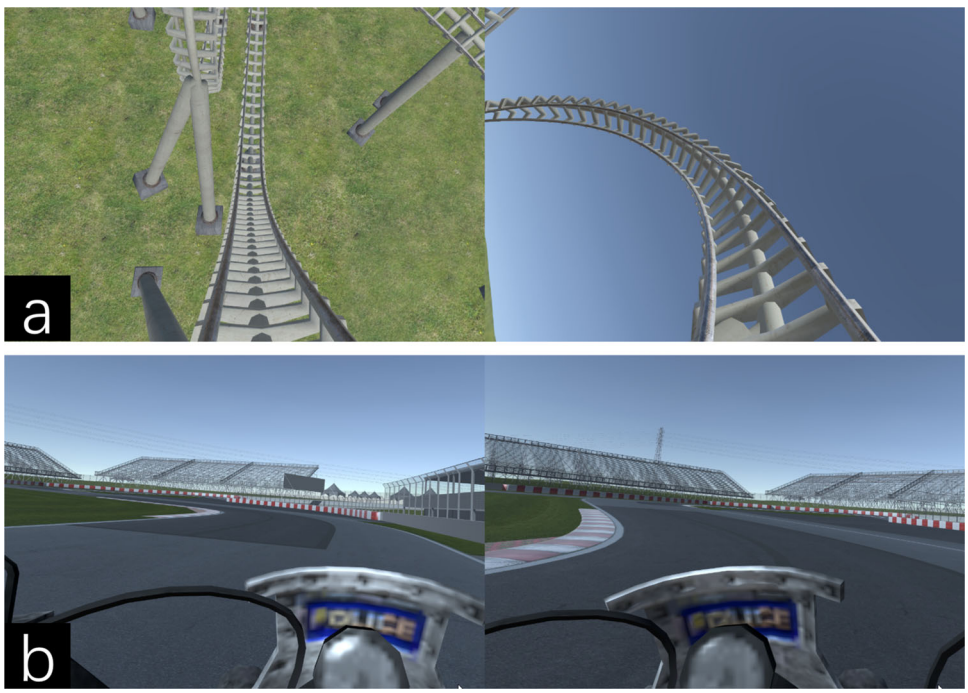

Fig. 10 Two VR scenarios that integrated AirWhisper: **a** Riding a roller coaster and **b** Riding a motorcycle

HMD. Controllers were not provided since user input was not required in this application. After a short familiarization with the environment, the roller coaster started. Participants rode the roller coaster for one whole course, passively experiencing a variety of postures accompanied by each feedback type during the process. In the second scene, riding a motorcycle, before the official test began, participants learned to use controllers to operate the motorcycle until they felt ready to start. When driving the motorcycle, participants were told to reach the finish line as soon as possible without crashing. There was a 10-minute break between the two applications. At the end of the experiment, participants were asked to fill out the questionnaires and be interviewed for additional comments. A total of 8 (2 (scenes) $\times$ 4 (feedback conditions)) trials were examined by each participant. The two applications were conducted in alternating order, and the sequence of the four conditions for each application was determined by a Latin Square approach to minimize carry-over effects. The whole experiment took about 50 min, including the introduction, rest, and interview.

5.3 Results

During the experiment, participants were asked to complete three questionnaires: E^2I, PQ, and SSQ. We used the Friedman Test to analyze the data and the Wilcoxon signed-rank test for post hoc analysis. For pairwise comparisons, we used the Bonferroni correction. The results show significant differences in participants' enjoyment and presence under different airflow conditions in the two scenarios but no significant differences in simulator sickness. We outline all results in detail in the following subsections.

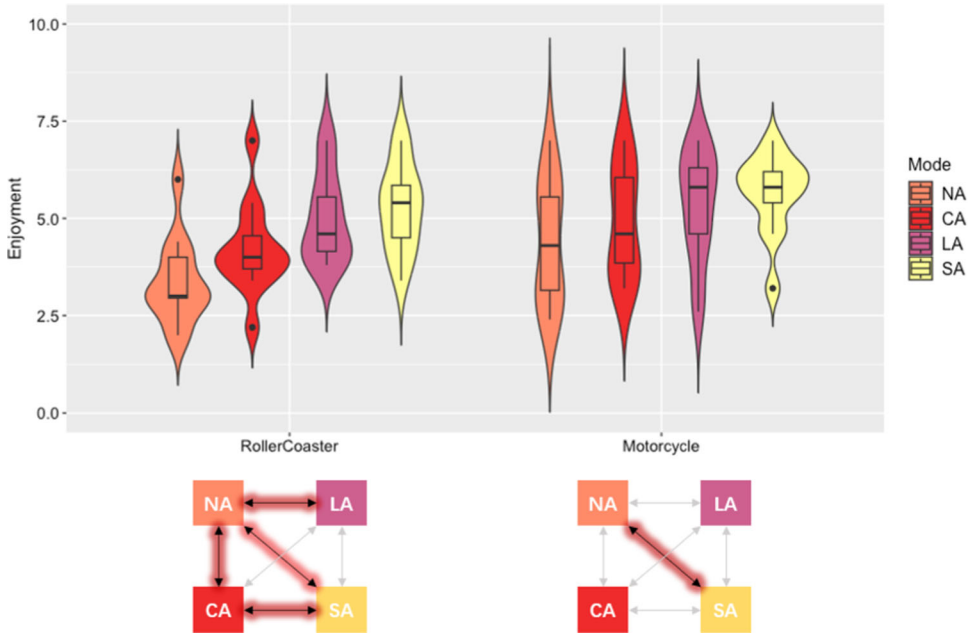

Fig. 11 Average of response scores for enjoyment questionnaire. Bold two-way arrows indicate a statistically significant difference between the two modes. NA: No Airflow. CA: Constant Airflow. LA: Linear-changing Airflow. SA: Step-changing Airflow

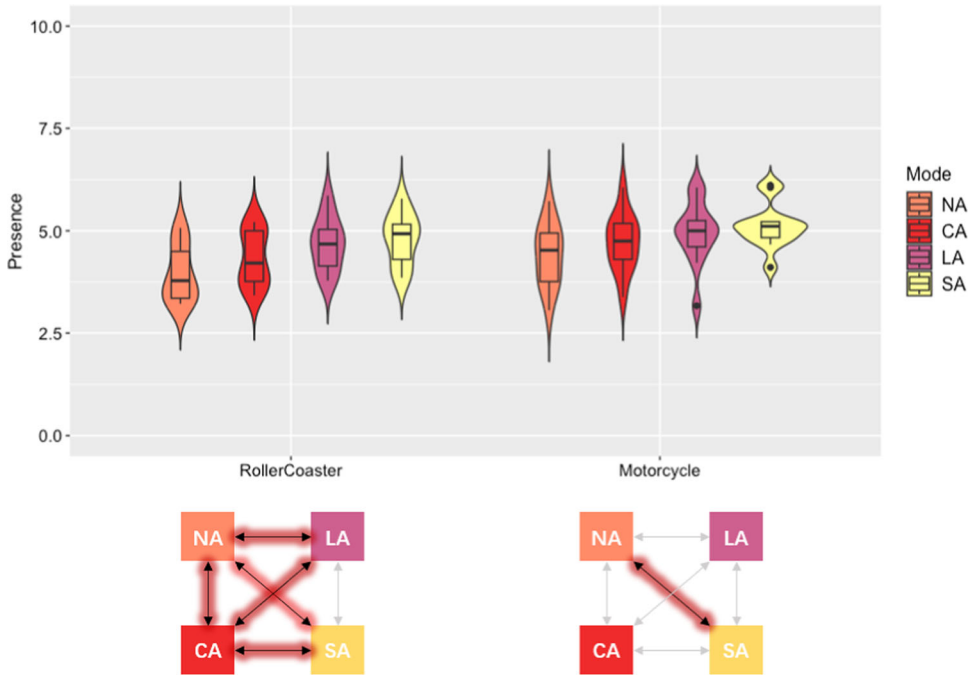

Fig. 12 Response scores for the presence questionnaire in **a** the roller coaster and **b** the motorcycle applications. Bold two-way arrows indicate a statistically significant difference between the two modes. NA: No Airflow. CA: Constant Airflow. LA: Linear-changing Airflow. SA: Step-changing Airflow

5.3.1 Enjoyment

Figure 11 shows the summary of the E^2I data. Employing the Friedman test to scrutinize within-subject differences across the conditions, both Roller Coaster conditions ($X^2(3) = 29.24$, $p < 0.001$) and Motorcycle conditions ($X^2(3) = 16.60$, $p < 0.001$) revealed a pronounced statistical significance. In the Roller Coaster scenario, participants exhibited a preference hierarchy, favoring the Step-changing Airflow condition ($M = 5.27$, $SD = 1.12$), then Linear-changing Airflow ($M = 5.02$, $SD = 1.16$), followed by Constant Airflow ($M = 4.22$, $SD = 1.19$), and least enjoyed was No Airflow ($M = 3.37$, $SD = 1.10$). Statistically significant contrasts were noted between No Airflow and each of the other three conditions (all $p < 0.05$) and between Constant and Step-changing Airflow ($p < 0.05$). However, the difference between Constant and Linear-changing Airflow and between Linear-changing and Step-changing Airflow was not statistically significant ($p > 0.05$).

For the Motorcycle scenario, a similar pattern of enjoyment scores was observed, with the Step-changing Airflow condition receiving the highest score ($M = 5.63$, $SD =$

1.03), succeeded by Linear-changing Airflow ($M = 5.33$, $SD = 1.43$), Constant Airflow ($M = 4.92$, $SD = 1.45$), and No Airflow ($M = 4.4$, $SD = 1.60$). Post-correction analysis revealed that the only significant difference in enjoyment was between No Airflow and Step-changing Airflow conditions ($p < 0.05$), while other pairwise comparisons remained statistically non-significant ($p > 0.05$).

5.3.2 Presence

Figure 12 shows the summary of the PQ data. The Friedman test has yielded statistically significant results for both Roller Coaster ($X^2(3) = 26.75$, $p < 0.001$) and Motorcycle ($X^2(3) = 14.89$, $p < 0.001$) scenes. In the Roller Coaster simulation, the presence scores revealed a preference for the Step-changing Airflow condition, which achieved the highest mean score ($M = 4.80$, $SD = 0.63$), followed by the Continuous-changing Airflow ($M = 4.68$, $SD = 0.65$), Constant Airflow ($M = 4.33$, $SD = 0.67$), and lastly No Airflow ($M = 3.95$, $SD = 0.69$). Notably, the comparison between the Linear-changing and Step-changing Airflow conditions did not exhibit a significant difference ($p > 0.05$), whereas all other comparisons did manifest significant differences ($p < 0.05$).

For the Motorcycle scene, the pattern of mean presence scores was akin to that of the Roller Coaster, with Step-changing Airflow once again receiving the highest mean score ($M = 5.12$, $SD = 0.55$). This was followed by Continuous-changing Airflow ($M = 4.95$, $SD = 0.78$), Constant Airflow ($M = 4.72$, $SD = 0.70$), and No Airflow ($M = 4.41$, $SD = 0.76$). However, in this scenario, a significant difference was only noted between the No Airflow and Step-changing Airflow conditions ($p < 0.05$), with the other comparisons not reaching statistical significance ($p > 0.05$).

5.3.3 Simulator sickness

The Friedman test for the simulator sickness data yielded the following results: Roller Coaster scene ($X^2(3) = 2.78$, $p = 0.427$), Motorcycle scene ($X^2(3) = 3.26$, $p = 0.353$). This indicates that there are no statistically significant differences in the simulator sickness levels experienced by participants across the different airflow conditions for both scenes.

5.4 Summary

The analyses showed that while the Simulator Sickness scores did not significantly differ across conditions, differences were found in the analysis of enjoyment and presence ratings. Based on the result of enjoyment and presence analysis, we got the following findings:

- In both interactive and non-interactive scenarios, any airflow feedback significantly improved presence and enjoyment over no airflow.
- For the non-interactive roller coaster, both dynamic airflow types (linear and step-changing) improved presence and enjoyment more than constant airflow.
- For the interactive motorcycle, only step-changing airflow significantly improved presence and enjoyment versus no airflow. Other airflow types did not differ significantly.
- Contrary to expectations, step-changing airflow did not outperform linear-changing airflow. Possible reasons are an inappropriate step-change design or scenarios better simulating linear changes.
- The impact of different airflow types depends on environmental interactivity. Dynamic airflow especially benefits non-interactive VR, while the most variable type (step-changing) aids interactive VR more.

In conclusion, integrating airflow feedback through AirWhisper greatly enhances users' VR experience, and the optimal airflow design should consider the interactive nature of the virtual environment.

6 Discussion

In this work, we evaluate AirWhisper's vision-airflow multimodal output performance and real-time dynamic feedback performance in terms of two evaluation criteria: the user's perceived accuracy of feedback performance and the user's experience, respectively. This section discusses the evaluation results, the causes of the results, and the contributions that can be generalized based on the results.

6.1 Reflection

In Study 1, we evaluated how single versus multimodal feedback impacted airflow perception, cognitive load, and user experience in VR using the AirWhisper device. Integrating visual cues with airflow significantly improved airflow perception accuracy, especially for lateral directions. This enhanced detection might result from multisensory integration processes that allow the brain to form a more comprehensive understanding by combining information from multiple modalities [49, 50]. Multimodal feedback also reduced the cognitive workload required for the task by distributing sensory processing [51]. Presenting information in a multisensory format can lessen the mental effort needed to interpret it. Moreover, users clearly preferred the multimodal feedback condition. This preference likely stems from the more natural and realistic experience it provides by better aligning with real-world interactions [52, 53]. The con-

gruence between simulated and actual sensory experiences enhances immersion and enjoyment. These findings validate AirWhisper's effectiveness in delivering an intuitive, user-friendly multisensory experience through its JND-calibrated control system. By systematically incorporating airflow sensations with congruent visual cues, it supports more precise spatial awareness, efficient cognitive processing, and an engaging VR experience overall. Overall, Study 1 highlights the value of multisensory designs for VR feedback systems.

In Study 2, we investigated the impact of different airflow feedback conditions on presence, enjoyment, and cognitive load in interactive versus non-interactive VR scenarios. We found that any airflow improved presence and enjoyment over no airflow in both contexts, while the beneficial effects of specific airflow types varied with interactivity. In the non-interactive roller coaster, both linear and step-changing dynamic airflows significantly outperformed constant airflow. This suggests dynamic changes alone enhanced the experience. However, in the interactive motorcycle scenario, only step-changing airflow significantly improved measures relative to no airflow. This may be because higher cognitive load limits environmental perception abilities [54, 55]. Under load, step-changing airflow with instantaneous changes was most detectable. Interestingly, enjoyment increased even when airflow inconsistencies were more apparent under load. This tolerance suggests users prioritize engagement over realism when cognition is taxed. Overall, these findings indicate optimal multimodal design depends on interactivity dynamics. AirWhisper supports a range of responsive airflow rendering tailored to scenario characteristics. Consideration of cognitive demands provides guidance for more user-centered VR experiences.

6.2 Limitations and future work

While AirWhisper provides an innovative and cost-effective solution for enhancing VR experiences, there are potential drawbacks and issues that may arise with long-term use. The frequent adjustment of the modular components, especially the 3D-printed supports and ball joints, could lead to wear and tear over time. Continuous use might result in the loosening of the joints or breakage of some plastic parts, necessitating periodic maintenance or replacement. Although the device is designed to be lightweight and adjustable, prolonged use might still lead to user fatigue or discomfort, especially around the attachment points. This is a common problem with current HMDs. In the future, when HMDs become smaller and weigh less, then fatigue issues will lessen as well.

In Study 2, we also observed an unexpected outcome where the presence of airflow did not significantly reduce simulator sickness. This contrasts with existing literature that highlights airflow's efficacy in mitigating discomfort. A primary factor in this discrepancy is the mode of airflow delivery. Previous studies have utilized large fans to generate whole-body airflow [15–19], differing from our use of a head-mounted airflow feedback interface. Head-mounted interfaces target the head and neck, regions more sensitive to airflow [43], creating a distinct experience compared to whole-body airflow perception. This difference may lead to varied effects on motion sickness. Notably, prior research employing headset-based airflow devices did not assess their impact using SSQ [14, 23, 24], making our study a first in this regard. Additionally, individual differences among participants and the subjective nature of self-reporting measurement methods like the SSQ could have influenced our results [56–58]. In general, as with any maturing technology, there is a continuous need for more diverse studies to investigate further the relationship between airflow and simulator sickness in VR environments, especially using non-subjective measurement methods.

Moreover, the (numerical) settings we used in Study 2 are derived from pilot tests performed in our target scenario and may not be applicable to other types of scenarios that have very different settings and users' expectations. Since we focus on studying how different airflow changing patterns can be applied to scenarios where movement and orientation changes take place, our results are applicable to scenarios with these features. It is outside of the scope of this paper to test all possible scenarios that VR environments can support. In the future, we plan to conduct further experiments with diverse types of scenarios to explore the effects of specific settings on users' perception and cognitive load.

7 Conclusion

In this paper, we introduced AirWhisper, a modular device capable of generating vision-airflow multimodal feedback calibrated to human perceptual characteristics. We conducted two studies To evaluate the usability and potential of AirWhisper. In study 1, we compared the effects of single versus multimodal feedback on airflow perception in virtual environments. The findings indicate that integrating visual cues with airflow information not only augments users' perceptual accuracy but also enriches the overall user experience while concurrently diminishing cognitive load. In Study 2, we tested four airflow variations across interactive and non-interactive VR scenarios. The results demonstrate that integrating airflow feedback through AirWhisper significantly enhances user experience in virtual reality, and the optimal design for airflow modification should consider the interactive characteristics of the virtual scenarios. Overall, this study introduces a novel, user-friendly modular device that provides visual-airflow multimodal outputs in virtual reality and provides ideas for human-centered multimodal interface design by evaluating the performance of this device

under different conditions in relation to the user's perceptual characteristics.

Acknowledgements The authors thank the participants who volunteered their time to join the experiments. We also thank the reviewers whose insightful comments and suggestions helped improve our paper. This work was partially funded by the Suzhou Municipal Key Laboratory for Intelligent Virtual Engineering (#SZS2022004) and the National Natural Science Foundation of China (#62207022).

References

1. Kim S, Billinghurst M, Kim K (2020) Multimodal interfaces and communication cues for remote collaboration. Springer, Berlin
2. Tatzgern M, Domhardt M, Wolf M, Cenger M, Emsenhuber G, Dinic R, Gerner N, Hartl A (2022) Airres mask: a precise and robust virtual reality breathing interface utilizing breathing resistance as output modality. In: Proceedings of the 2022 CHI conference on human factors in computing systems, pp 1–14
3. Chai K, Li Y, Yu L, Liang H-N (2023) Hapticbox: designing handheld thermal, wetness, and wind stimuli for virtual reality. In: 2023 IEEE conference on virtual reality and 3D user interfaces abstracts and workshops (VRW), pp. 873–874 . https://doi.org/10.1109/VRW58643.2023.00279
4. Sun Z, Zhu M, Shan X, Lee C (2022) Augmented tactile-perception and haptic-feedback rings as human-machine interfaces aiming for immersive interactions. Nat Commun 13(1):5224
5. Wang X, Monteiro D, Lee L-H, Hui P, Liang H-N (2022) Vibroweight: simulating weight and center of gravity changes of objects in virtual reality for enhanced realism. In: 2022 IEEE haptics symposium (HAPTICS), pp 1–7. https://doi.org/10.1109/HAPTICS52432.2022.9765609
6. Zhao Z, Li Y, Liang H-N (2023) Leanon: simulating balance vehicle locomotion in virtual reality. In: 2023 IEEE international symposium on mixed and augmented reality (ISMAR), pp 415–424 . https://doi.org/10.1109/ISMAR59233.2023.00056
7. Fang H, Guo J, Wu H (2022) Wearable triboelectric devices for haptic perception and vr/ar applications. Nano Energy 96:107112
8. Bai H, Li S, Shepherd RF (2021) Elastomeric haptic devices for virtual and augmented reality. Adv Func Mater 31(39):2009364
9. Ahmed KS (2003) Comfort in urban spaces: defining the boundaries of outdoor thermal comfort for the tropical urban environments. Energy Build 35(1):103–110
10. Andrade H, Alcoforado M-J, Oliveira S (2011) Perception of temperature and wind by users of public outdoor spaces: relationships with weather parameters and personal characteristics. Int J Biometeorol 55:665–680
11. Knez I, Thorsson S (2006) Influences of culture and environmental attitude on thermal, emotional and perceptual evaluations of a public square. Int J Biometeorol 50:258–268
12. Song S, Noh G, Yoo J, Oakley I, Cho J, Bianchi A (2015) Hot & tight: exploring thermo and squeeze cues recognition on wrist wearables. In: Proceedings of the 2015 ACM international symposium on wearable computers, pp 39–42
13. Lee J (2017) Wind tactor: An airflow-based wearable tactile display. In: Adjunct proceedings of the 30th annual ACM symposium on user interface software and technology, pp 91–94
14. Ranasinghe N, Jain P, Karwita S, Tolley D, Do EY-L (2017) Ambiotherm: enhancing sense of presence in virtual reality by simulating real-world environmental conditions. In: Proceedings of the 2017 CHI conference on human factors in computing systems, pp 1731–1742
15. Matviienko A, Müller F, Zickler M, Gasche LA, Abels J, Steinert T, Mühlhäuser M (2022) Reducing virtual reality sickness for cyclists in vr bicycle simulators. In: Proceedings of the 2022 CHI conference on human factors in computing systems, pp 1–14
16. Paroz A, Potter LE (2021) Investigating external airflow and reduced room temperature to reduce virtual reality sickness. In: Proceedings of the 33rd Australian conference on human-computer interaction, pp 198–207
17. Harrington J, Williams B, Headleand C (2019) A somatic approach to combating cybersickness utilising airflow feedback. In: Vidal FP, Tam GKL, Roberts JC (eds) Computer graphics and visual computing (CGVC). https://doi.org/10.2312/cgvc.20191256
18. D'Amour S, Bos JE, Keshavarz B (2017) The efficacy of airflow and seat vibration on reducing visually induced motion sickness. Exp Brain Res 235:2811–2820
19. Suzuki Y, Yem V, Hirota K, Amemiya T, Kitazaki M, Ikei Y (2019) Airflow presentation method for turning motion feedback in VR environment. In: ICAT-EGVE 2019 - international conference on artificial reality and telexistence and eurographics symposium on virtual environments - posters and demos. https://doi.org/10.2312/egve.20191295
20. Kim K, Schubert R, Hochreiter J, Bruder G, Welch G (2019) Blowing in the wind: increasing social presence with a virtual human via environmental airflow interaction in mixed reality. Comput Graph 83:23–32
21. Hülsmann F, Fröhlich J, Mattar N, Wachsmuth I (2014) Wind and warmth in virtual reality: implementation and evaluation. In: Proceedings of the 2014 virtual reality international conference, pp 1–8
22. Moon T, Kim GJ (2004) Design and evaluation of a wind display for virtual reality. In: Proceedings of the ACM symposium on virtual reality software and technology, pp 122–128
23. Rietzler M, Plaumann K, Kränzle T, Erath M, Stahl A, Rukzio E (2017) Vair: Simulating 3d airflows in virtual reality. In: Proceedings of the 2017 CHI conference on human factors in computing systems. CHI '17, pp. 5669–5677. Association for Computing Machinery, New York, NY, USA. https://doi.org/10.1145/3025453.3026009
24. Tseng C-M, Chen P-Y, Lin SC, Wang Y-W, Lin Y-H, Kuo M-A, Yu N-H, Chen MY (2022) Headwind: enhancing teleportation experience in vr by simulating air drag during rapid motion. In: Proceedings of the 2022 CHI conference on human factors in computing systems, pp 1–11
25. Monteiro D, Liang H-N, Wang X, Xu W, Tu H (2021) Design and development of a low-cost device for weight and center of gravity simulation in virtual reality. In: Proceedings of the 2021 international conference on multimodal interaction. ICMI '21, pp 453–460. Association for computing machinery, New York, NY, USA. https://doi.org/10.1145/3462244.3479907
26. Cai S, Ke P, Narumi T, Zhu K (2020) Thermairglove: a pneumatic glove for thermal perception and material identification in virtual reality. In: 2020 IEEE conference on virtual reality and 3D user interfaces (VR), pp 248–257. IEEE
27. Burdea G, Richard P, Coiffet P (1996) Multimodal virtual reality: input-output devices, system integration, and human factors. Int J Human Comput Interact 8(1):5–24
28. Yokokohji Y, Hollis RL, Kanade T (1999) Wysiwyf display: a visual/haptic interface to virtual environment. Presence 8(4):412–434
29. Schwind V, Lin L, Di Luca M, Jörg S, Hillis J (2018) Touch with foreign hands: The effect of virtual hand appearance on visual-haptic integration. In: Proceedings of the 15th ACM symposium on applied perception, pp 1–8
30. Gibbs JK, Gillies M, Pan X (2022) A comparison of the effects of haptic and visual feedback on presence in virtual reality. Int J Hum Comput Stud 157:102717

31. Wu E, Piekenbrock M, Nakumura T, Koike H (2021) Spinpong-virtual reality table tennis skill acquisition using visual, haptic and temporal cues. IEEE Trans Visual Comput Graphics 27(5):2566–2576
32. Sodhi R, Poupyrev I, Glisson M, Israr A (2013) Aireal: interactive tactile experiences in free air. ACM Trans Graph (TOG) 32(4):1–10
33. Tsalamlal MY, Ouarti N, Martin J-C, Ammi M (2015) Haptic communication of dimensions of emotions using air jet based tactile stimulation. J Multimodal User Interfaces 9:69–77
34. Liu S-H, Yen P-C, Mao Y-H, Lin Y-H, Chandra E, Chen MY (2020) Headblaster: a wearable approach to simulating motion perception using head-mounted air propulsion jets. ACM Trans Graph (TOG) 39(4):84
35. Stern MK, Johnson JH (2010) Just noticeable difference. In: The corsini encyclopedia of psychology, pp 1–2. https://doi.org/10.1002/9780470479216.corpsy048
36. Park J, Bennis M (2018) Urllc-embb slicing to support VR multimodal perceptions over wireless cellular systems. In: 2018 IEEE global communications conference (GLOBECOM), pp. 1–7. IEEE
37. Lee Y, Jang I, Lee D (2015) Enlarging just noticeable differences of visual-proprioceptive conflict in VR using haptic feedback. In: 2015 IEEE world haptics conference (WHC), pp 19–24. IEEE
38. Tsai H-R, Chen B-Y (2019) Elastimpact: 2.5 d multilevel instant impact using elasticity on head-mounted displays. In: Proceedings of the 32nd annual ACM symposium on user interface software and technology, pp 429–437
39. Junput B, Wei X, Jamone L (2019) Feel it on your fingers: dataglove with vibrotactile feedback for virtual reality and telerobotics. In: Towards autonomous robotic systems: 20th annual conference, TAROS 2019, London, UK, July 3–5, 2019, Proceedings, Part I 20, pp 375–385. Springer
40. Ryu N, Lee W, Kim MJ, Bianchi A (2020) Elastick: a handheld variable stiffness display for rendering dynamic haptic response of flexible object. In: Proceedings of the 33rd annual ACM symposium on user interface software and technology, pp 1035–1045
41. Pluijms JP, Cañal-Bruland R, Bergmann Tiest WM, Mulder FA, Savelsbergh GJ (2015) Expertise effects in cutaneous wind perception. Attent Percept Psychophys 77:2121–2133
42. Tsalamlal MY, Ouarti N, Ammi M (2013) Psychophysical study of air jet based tactile stimulation. In: 2013 world haptics conference (WHC), pp 639–644. IEEE
43. Lee J, Lee G (2016) Designing a non-contact wearable tactile display using airflows. In: Proceedings of the 29th annual symposium on user interface software and technology. UIST '16, pp 183–194. Association for Computing Machinery, New York, NY, USA. https://doi.org/10.1145/2984511.2984583
44. Hart SG, Staveland LE (1988) Development of nasa-tlx (task load index): results of empirical and theoretical research. Advances in Psychology, vol 52. Elsevier, Amsterdam, pp 139–183
45. Brooke J et al (1996) Sus-a quick and dirty usability scale. Usability Evaluat Ind 189(194):4-7
46. Witmer BG, Singer MJ (1998) Measuring presence in virtual environments: a presence questionnaire. Presence 7(3):225–240
47. Lin J-W, Duh HB-L, Parker DE, Abi-Rached H, Furness TA (2002) Effects of field of view on presence, enjoyment, memory, and simulator sickness in a virtual environment. In: Proceedings IEEE virtual reality 2002, pp 164–171. IEEE
48. Kennedy RS, Lane NE, Berbaum KS, Lilienthal MG (1993) Simulator sickness questionnaire: an enhanced method for quantifying simulator sickness. Int J Aviat Psychol 3(3):203–220
49. Spence C, Driver J (2004) Crossmodal space and crossmodal attention. Oxford University Press, Oxford
50. Wu Z, Shi R, Li Z, Jiang M, Li Y, Yu L, Liang H-N (2022) Examining cross-modal correspondence between ambient color and taste perception in virtual reality. Front Virtual Real 3:1056782. https://doi.org/10.3389/frvir.2022.1056782
51. Wickens CD, Helton WS, Hollands JG, Banbury S (2021) Engineering psychology and human performance. Routledge, London
52. Slater M, Wilbur S (1997) A framework for immersive virtual environments (five): speculations on the role of presence in virtual environments. Presence Teleoper Virtual Environ 6(6):603–616
53. Dinh HQ, Walker N, Hodges LF, Song C, Kobayashi A (1999) Evaluating the importance of multi-sensory input on memory and the sense of presence in virtual environments. In: Proceedings IEEE virtual reality (Cat. No. 99CB36316), pp 222–228. IEEE
54. Lavie N (1995) Perceptual load as a necessary condition for selective attention. J Exp Psychol Hum Percept Perform 21(3):451
55. Styles E (2006) The psychology of attention. Psychology Press, London
56. Biswas N, Mukherjee A, Bhattacharya S (2024) "Are you feeling sick?"-a systematic literature review of cybersickness in virtual reality. ACM Comput Surv 56(11):1–38. https://doi.org/10.1145/3670008
57. Wang J, Liang H-N, Monteiro D, Xu W, Xiao J (2023) Real-time prediction of simulator sickness in virtual reality games. IEEE Trans Games 15(2):252–261. https://doi.org/10.1109/TG.2022.3178539
58. Monteiro D, Liang H-N, Tang X, Irani P (2021) Using trajectory compression rate to predict changes in cybersickness in virtual reality games. In: 2021 IEEE international symposium on mixed and augmented reality (ISMAR), pp 138–146. https://doi.org/10.1109/ISMAR52148.2021.00028